




Original research

# Autoimmune gastritis: long-term natural history in naïve *Helicobacter pylori*-negative patients

Massimo Rugge <sup>1,2</sup>, Ludovica Bricca,<sup>1</sup> Stefano Guzzinati,<sup>2</sup> Diana Sacchi,<sup>3</sup> Marco Pizzi,<sup>1</sup> Edoardo Savarino,<sup>3</sup> Fabio Farinati,<sup>3</sup> Manuel Zorzi <sup>2</sup>, Matteo Fassan,<sup>1,4</sup> Angelo Paolo Dei Tos,<sup>1</sup> Peter Malfertheiner,<sup>5</sup> Robert M Genta,<sup>6,7</sup> David Y Graham <sup>7</sup>

<sup>1</sup>Department of Medicine - DIMED, Ringgold ID 9308, Padova, Veneto, Italy

<sup>2</sup>Veneto Tumor Registry, Azienda Zero, Padova, Veneto, Italy

<sup>3</sup>Department of Surgery, Oncology and Gastroenterology, University of Padova, Ringgold ID 9308, Padova, Italy

<sup>4</sup>Veneto Institute of Oncology - IOV - IRCCS, Padova, Italy

<sup>5</sup>Radiology, Ludwig Maximilians University Munich, Munchen, Germany

<sup>6</sup>Department of Pathology, Baylor College of Medicine Houston, Texas, USA, Houston, Texas, USA

<sup>7</sup>Department of Medicine, Michael E. De Bakey VA Medical Center, Baylor College of Medicine Houston, Houston, Texas, USA

## Correspondence to

Professor Massimo Rugge, Department of Medicine - DIMED, Università degli Studi di Padova, Padova 35121, Veneto, Italy; massimo.rugge@unipd.it

Received 11 May 2022

Accepted 15 June 2022

Published Online First

30 June 2022



► <http://dx.doi.org/10.1136/gutjnl-2022-328068>



© Author(s) (or their employer(s)) 2023. No commercial re-use. See rights and permissions. Published by BMJ.

**To cite:** Rugge M, Bricca L, Guzzinati S, et al. *Gut* 2023;**72**:30–38.

## ABSTRACT

**Objective** Autoimmune gastritis (AIG) is an immunomediated disease targeting parietal cells, eventually resulting in oxyntic-restricted atrophy. This long-term follow-up study aimed at elucidating the natural history, histological phenotype(s), and associated cancer risk of patients with AIG consistently tested *H. pylori*-negative (naïve *H. pylori*-negative subjects).

**Design** Two-hundred eleven naïve *H. pylori*-negative patients (tested by serology, histology, molecular biology) with AIG (F:M=3.15:1; p<0.001) were prospectively followed up with paired biopsies (T1 vs T2; mean follow-up years:7.5 (SD:4.4); median:7). Histology distinguished non-atrophic versus atrophic AIG. Atrophy was further subtyped/scored as non-metaplastic versus metaplastic (pseudopyloric (PPM) and intestinal (IM)). Enterochromaffin-like-cell (ECL) status was categorised as diffuse versus adenomatoid hyperplasia/dysplasia, and type 1 neuroendocrine tumours (Type1-NETs).

**Results** Over the long-term histological follow-up, AIG consistently featured oxyntic-predominant-mononuclear inflammation. At T1, PPM-score was greater than IM (200/211 vs 160/211, respectively); IM scores increased from T1 to T2 (160/211 to 179/211), with no changes in the PPM prevalence (T1=200/211; T2=201/211). At both T1/T2, the prevalence of OLGA-III-stage was <5%; no Operative Link on Gastritis Assessment (OLGA)-IV-stage occurred. ECL-cell-status progressed from diffuse to adenomatoid hyperplasia/dysplasia (T1=167/14 vs T2=151/25). Type1-NETs (T1=10; T2=11) always coexisted with extensive oxyntic-atrophy, and ECL adenomatoid-hyperplasia/dysplasia. No excess risk of gastric or other malignancies was found over a cumulative follow-up time of 10 541 person years, except for (marginally significant) thyroid cancer (SIR=3.09; 95% CI 1.001 to 7.20).

**Conclusions** Oxyntic-restricted inflammation, PPM (more than IM), and ECL-cell hyperplasia/neoplasia are the histological AIG hallmarks. Compared with the general population, corpus-restricted inflammation/atrophy does not increase the GC risk. The excess of GC risk reported in patients with AIG could plausibly result from unrecognised previous/current *H. pylori* comorbidity.

## INTRODUCTION

Gastric inflammatory conditions have traditionally been classified based on their aetiology into host and environment related.<sup>1 2</sup> Worldwide, the

### WHAT IS ALREADY KNOWN ON THIS SUBJECT?

⇒ Autoimmune gastritis (AIG) is an immunomediated inflammation of oxyntic mucosa, mostly diagnosed in its atrophic stage. Due to the possible concurrence of previous or current *H. pylori* infection, the risk of AIG-associated gastric cancer (GC) remains unclear.

### WHAT ARE THE NEW FINDINGS?

⇒ When previous or current *H. pylori* infection is rigorously excluded, the long-term follow-up of AIG does not reveal any excess risk for malignancy, except for thyroid cancers. In the natural history of AIG, the initial extensive pseudopyloric metaplasia is slowly replaced by focal gland intestinalisation.  
⇒ Enterochromaffin-like-cell hyperplasia, an essential feature of AIG, progresses from diffuse to adenomatoid, the latter being significantly associates with type 1 neuroendocrine tumours.

### HOW MIGHT IT IMPACT ON CLINICAL PRACTICE IN THE FORESEEABLE FUTURE?

⇒ In naïve *H. pylori*-negative patients, neuroendocrine neoplasia, not GC secondary prevention, prioritises the clinical, endoscopic and histopathological surveillance of AIG.

environmental aetiology is by far the most prevalent, with *Helicobacter pylori* (*H. pylori*) being the most common agent of gastritis. The prototype of host-related, non-self-limiting gastritis is autoimmune gastritis (AIG), a corpus-restricted progressive inflammatory process that specifically targets the oxyntic mucosa.<sup>3–5</sup> Over the course of decades, oxyntic glands are destroyed and replaced by a morphologically and functionally atrophic metaplastic mucosa, while the antrum remains essentially unaffected by any inflammatory involvement and its resulting atrophy. As the destruction of the oxyntic mucosa advances, hypo- and then achlorhydria develop and the production of intrinsic factor (IF) decreases or vanishes. These changes are reflected morphologically by hyperplasia and neoplasia of the enterochromaffin-like (ECL) cells of the gastric corpus and functionally by an impaired absorption of cobalamin, which eventually results in the syndrome known as pernicious anaemia.

**Table 1** Patients with AIG: demographics and clinicopathological profile

Variable	T1 211 patients	Female 160 (75.8%)	Male 51 (24.2%)	T2 211 patients	Female 160 (75.8%)	Male 51 (24.2%)
Age: Mean (SD); median	55.7 (1 4.1); 56	54.5 (14.3); 55	59.7 (13.0); 63	63.3 (13.3); 64	62.2 (13.5); 62	66.5 (12.5); 67
<i>H. pylori</i> status (serology, histology, molecular biology on tissue samples)	All negative	160	51	All negative	160	51
Follow-up (years): mean (SD); median				7.5 (4.4); 7	7.7 (4.5); 7	7.0 (4.1); 6
OLGA staging						
0	8 (3.8%)	8	0	7 (3.3%)	6	1
I	23 (10.9%)	19	4	19 (9.0%)	16	3
II	179 (84.8%)	132	47	175 (82.9%)	129	46
III	1 (0.5%)	1	0	10 (4.7%)	9	1
IV	0	0	0	0	0	0
IEN						
Absent	210			209		
Low grade	1 (FAP)			2 (1 FAP)		
High grade	0			0		
ECL status						
Within normal limits	20	15	5	24	19	5
Diffuse hyperplasia linear/micronodular	167	130	37	151	109	42
Adenomatoid hyperplasia/dysplasia	14	11	3	25	22	3
Type1-NET	10	4	6	11	10	1

ECL, enterochromaffin like cells; FAP, familial adenomatous polyposis; IEN, intraepithelial neoplasia; T1, time of the index biopsy set; T2, time of the last check-up; Type1-NET, type 1 neuroendocrine tumours.

Since its early descriptions in the XIX century, AIG (particularly when associated with pernicious anaemia) has been considered as a gastric precancerous condition.<sup>6–10</sup> However, essentially all studies reporting an increased cancer risk associated with AIG were performed either in the pre-*H. pylori* era (before *H. pylori* was known to exist) or in patients who, unbeknownst to the investigators, may have had *H. pylori* gastritis before atrophy developed and cleared the infection. Such cohorts of subjects with unknown concurrent or previous *H. pylori* infection were inadequate to provide accurate information on the risk of gastric cancer (GC) associated with the immunomodulated mechanism of mucosal atrophy at the root of AIG.<sup>11</sup>

Therefore, while the spectrum of neuroendocrine gastric hyperplastic and neoplastic proliferations is well documented, the risk for GC associated with AIG remains uncertain.

To gather reliable data on the association between ‘pure AIG’ (that is, not associated with even incidental *H. pylori* infection), we designed a prospective single-centre long-term study of AIG based on rigorous clinical, serological and histopathological criteria. At enrolment, all patients had Sydney System-compliant biopsy sets (the ‘index biopsy’) considered characteristic of AIG, with corpus-restricted atrophic metaplastic gastritis, ECL-cell hyperplasia, and an essentially normal antral mucosa.<sup>12–15</sup> A second set of paired biopsies was obtained from all patients at least 12 months after the index biopsy. At the time of enrolment, no patient had serological, histological or molecular evidence of either previous or current *H. pylori* infection, and none had a known history of previously eradicated infection.

The primary aim of this study was to define the natural history of pure AIG and to elucidate its potential neoplastic evolution in the absence of *H. pylori* infection.<sup>16</sup>

## PATIENTS AND METHODS

### Patients: inclusion criteria

This monoinstitutional study includes a cohort of 211 consecutive patients with clinical, serological and histological features

consistent with AIG (table 1). In all patients, previous or current *H. pylori* infection was excluded by serology, histology and molecular biology testing, and all underwent at least two paired endoscopies with biopsies. All patients were Caucasian, native of Veneto, a northeastern Italian Region.

Inclusion criteria were as follows (table 1):

- ▶ age over 18 years;
- ▶ no clinical history of oesophago-gastric malignancies;
- ▶ a clinical syndrome consistent with AIG, including serological testing for parietal cell and/or IF autoantibodies (Autozyme IFab; Cambridge Life Sciences, Ely, UK);
- ▶ follow-up ≥ 12 months, including at least two EGDs, associated with paired biopsy sets (T1: index biopsy set; T2: last biopsy set);
- ▶ a gastric biopsy protocol including samples from the antrum, the *incisura angularis*, and the oxyntic mucosa. Samples from the *incisura* were submitted in the same vial as the antral specimens. At each EGD, additional specimens were obtained, and separately submitted, from any discrete lesion;
- ▶ no evidence of previous or current *H. pylori* infection, as excluded by serology testing, histology, and molecular biology assay (as detailed below);
- ▶ written informed consent to undergo the EGD with biopsies and to allow deidentified information to be used for research purposes.

By protocol, patients were asked to discontinue proton pump inhibitor therapy 2 weeks before each EGD. All patients meeting the inclusion criteria between the years 2002–2020 were included in the study population.

### Biopsy sampling protocol and histological criteria

In all cases, at least two sets of paired biopsy specimens were available (mean=2.7 (SD=0.79); median 3). At T1, the biopsy sets obtained from the oxyntic and mucosecreting (antral) mucosa included a mean of 4.4 (SD:3; median 3) and 3.5 (SD:1.7; median 3) biopsy samples, respectively. At T2, the

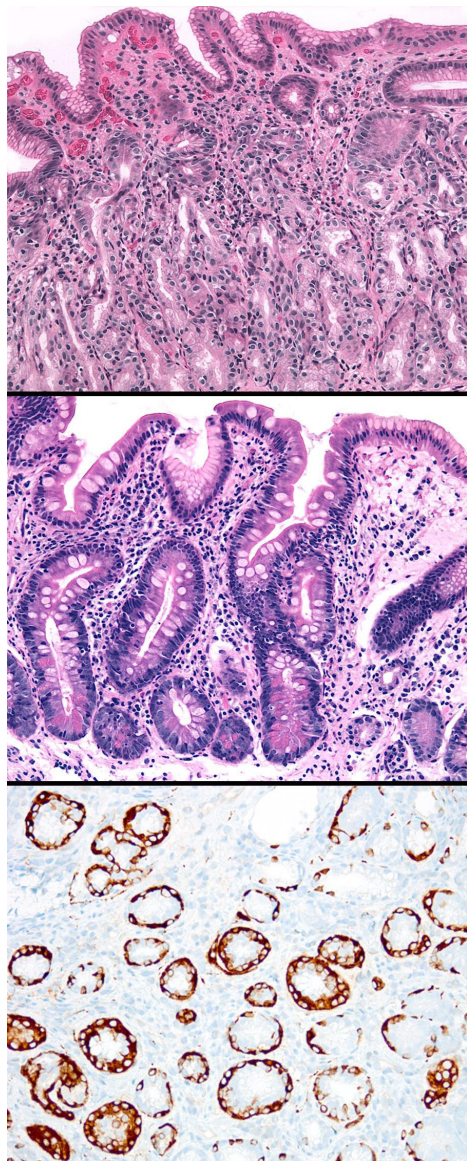


**Figure 1** Panel A: oxyntic mucosa biopsy specimen featuring early autoimmune gastritis (AIG). The linear architecture of the oxyntic glands is still discernible; some pseudopyloric cells alternate native epithelia, and there is a sparse mononuclear infiltrate. Panel B: advanced atrophic AIG: the entire oxyntic mucosa is involved by atrophy and intestinal metaplasia. Large parts of the lamina propria are expanded by fibrous tissue separating the glandular coils from the muscularis mucosae. Intestinalised glands exhibit complete IM phenotype. Panel C: immunohistochemical staining with chromogranin A or synaptophysin (depicted here) shows extensive linear ECL-cell hyperplasia as well as rare focal micronodular hyperplastic foci. These are constant features of the advanced stages of AIG.

biopsy set obtained from the oxyntic and antral mucosa included a mean of 5.5 (SD:3.1; median 5) and 4.2 (SD:2.0; median 4) biopsy samples, respectively.

A histopathological examination of either the original slides or serial sections (4–5  $\mu$ m thick) obtained from the original formalin-fixed paraffin-embedded tissue samples was performed in each case after the study was closed. In all cases, the following stains and immunostains were available for each sample: (1) H&E; (2) Giemsa stain modified for *H. pylori* detection; (3) an immunohistochemical (IHC) stain for *H. pylori* detection.<sup>17 18</sup>

On a subset of oxyntic samples, IHC was also performed for: (1) chromogranin A (chromogranin A; clone DAK-A3; DAKO); (2) Ki67/Mib1 expression (DAKO, Glostrup, Denmark). Appropriate negative and positive controls were run with each IHC batch.

Only cases with either corpus-restricted or corpus-predominant inflammation (as defined in the updated Sydney System) were accepted as being consistent with AIG. In both antral and oxyntic specimens, gastritis was primarily classified as non-atrophic versus atrophic (figure 1).<sup>19 20</sup>

The mononuclear inflammatory infiltrate (lymphocytes, plasma cells, macrophages) within the lamina propria was graded using a three-tiered scale: (1) within normal limits; (2) low grade; (3) high grade, the latter even including follicular or nodular lymphoplasmacytic aggregates. In these cohort, no cases of high-grade polymorphs' (PMN) infiltrate were ever detected (ie, intraglandular PMNs clusters within the glandular lumen and/or within the lamina propria ('activity')); therefore, PMN infiltrates were simply scored as present versus absent.

The histological phenotypes of the lesions included in the atrophy spectrum were: (1) non-metaplastic atrophy; (2) pseudopyloric metaplasia (PPM)<sup>8 21–23</sup>; and (3) intestinal metaplasia (IM) (figure 1).<sup>24 25</sup> Each atrophy variant was scored as a percentage of the available tissue specimens obtained from the same gastric mucosal compartment (ie, set of the biopsy specimens obtained from oxyntic mucosa vs biopsy set obtained from mucosecreting mucosa, including specimens from the incisura). The OLGA staging system for gastritis was applied according to the recommended criteria.<sup>26 27</sup>

On the oxyntic mucosa samples, the status of enterochromaffin like cell (ECL-cell) was established as suggested by Vanoli *et al*<sup>28</sup>: (1) ECL-cell population within normal limits; (2) diffuse linear and/or micronodular hyperplasia (figure 1); (3) adenomatoid hyperplasia, and the so-called 'dysplasia' (enlarged/fused micronodules adenomatous/fused micronodules even coexisting with strictly adjacent perinodular ECL); and (4) neoplasia (Type1 neuroendocrine tumours (NET)), intramucosal or invasive.

Both intraepithelial and invasive epithelial neoplastic lesions were assessed and classified according to the current international recommendations.<sup>29 30</sup>

A pathologist with elective experience in GI pathology (DS), blinded to all endoscopic and clinical information, oversaw the histological assessment. The interobserver agreement for all the variables evaluated (*H. pylori*-status; atrophy score, inflammatory infiltrate, activity, ECL-cell status) was calculated in a sample of 78 randomly selected biopsy sets. The diagnostic consistency between two pathologists (DS and MR) for atrophy, inflammatory mucosal scores, ECL-status assessment, and intraepithelial neoplasia ((IEN) synonym: dysplasia) resulted in a  $\kappa$ -statistics value ranging from 0.76 and 0.88 (very good to excellent).<sup>31</sup>

#### Assessment of *H. pylori* status: serology, histology and molecular biology testing

Serological testing for *H. pylori* status was based on *H. pylori* specific IgG antibodies detection which detect both current and previous bacterial infection.<sup>32–35</sup>

Histologically, *H. pylori*-negative status was established using both the modified Giemsa stain and an anti-*H. pylori* immunohistochemical stain (VENTANA anti-*H. pylori* SP48 Rabbit monoclonal; Ventana-Roche). In all patients, *H. pylori* status was further assessed by molecular techniques.<sup>36 37</sup> Real-time PCR was applied on DNA extracted by a pool of antral and oxyntic

formalin-fixed paraffin-embedded tissue samples. The detection system for *H. pylori* DNA based was applied (PhoenixDx *H. pylori*; Procomcure Biotech GmbH-Austria) according to the manufacturer's protocol. The analytical sensitivity of the method is seven target copies per PCR reaction. All tests were run with positive and negative controls as per test protocol. Only patients who tested negative for all three diagnostic tests were included.

### Incident primary epithelial malignancies

The cancer history of all the study patients was checked through record linkage with the database of the regional cancer registry (Veneto Cancer Registry (RTV)),<sup>38</sup> and we considered cancers diagnosed both before and after the diagnosis of AIG. Non-malignant tumours and non-melanoma skin cancers were not considered.

### Statistics

All statistical analyses were performed using the SAS software.<sup>39</sup> Comparisons of continuous data between two or more groups were performed using the *t*-test and analysis of variance, respectively. Fisher's exact test was used to evaluate dependence between categorical variables. Statistical significance was set at  $p < 0.05$ . Standardised incidence ratio (SIR) for malignancies was calculated in order to estimate the excess in cancer risk among the study patients. The study person years were defined by summing the follow-up time of all patients, who participated from the age of 18 and up to the date of cancer diagnosis, the date of death, or the end of the study follow-up (31 December 2020), whichever came first. The expected number of cancers was assessed by applying the regional sex-specific, age-specific and period-specific incidence rates published by the Regional Cancer registry to the study person years. SIR was calculated as the observed-to expected ratio, with 95% CI based on exact values of Poisson.

## RESULTS

### Demographics, comorbidities and follow-up

During the period of the study (2002–2020), AIG was suspected in 538 patients, based on clinical presentation, endoscopic findings, or histological pattern of gastritis. When all inclusion and exclusion criteria were met, 211 patients were included in the analysis.

All 211 patients were Caucasian (F:M=3.15:1;  $p < 0.001$ ) and 198 of them were native of the Veneto region. At the time of the index endoscopy (T1), women (160/211) were significantly younger than men (mean age: 54.5 (SD 14.3); median: 55; males: 59.7 (SD: 13.0); median 63;  $p = 0.02$ ) (table 1).

Clinical information on comorbidities was available for a subset of the study population. Haematological laboratory data at both T1 and T2 were available in 162/211 patients: normocytic or macrocytic anaemia was detected in 72/162 subjects at T1, and in 81/162 subjects at T2. Histologically confirmed, presumably immune-mediated, GI disorders coexisted in 22/139 patients (12 coeliac disease; 4 UC, 3 Crohn disease; 2 eosinophilic esophagitis, and 1 primary biliary cirrhosis). Serologically proven autoimmune thyroiditis was present in 58/153 patients, of whom 50 (86.2%) were women.

### Histology

*Grading of the inflammatory lesions:* in all 211 paired biopsy samples inflammation was histologically scored separately in the proximal (oxyntic, table 2) and distal (mucosecreting antral, or incisural; table 2) mucosal compartments. At both T1 and T2, all oxyntic mucosa samples showed a mononuclear inflammatory population above the normal limits. High-grade mononuclear infiltrate (including lymphoid nodules, and follicles) was found at enrolment in 29.2% of the subjects and at the last available biopsy check-up in 39.8% of them. The scores for mononuclear inflammation in the oxyntic mucosa underwent no change from T1 to T2 in 120 of 211 cases (56.9%), increased in 57/211 patients (27.0%), and decreased in 34/211 subjects (16.1%) (table 2;  $p = 0.43$ ). Sparse PMNs were present in the oxyntic inflammatory infiltrate in 31.3% of the subjects at T1 and in 35.0% at T2 ( $p = 0.54$ ; not shown in table).

In the biopsy sets obtained from the distal gastric compartment (table 2), the mononuclear infiltrate was within normal limits in 186/211 (88.1%), and 171/211 (88.0%), at T1 and T2, respectively. Low-grade mononuclear infiltration was detected in the antral mucosa of 25/211 (11.8%) patients at T1 and in 40/211 (18.9%) at T2. High-grade mononuclear inflammation was not detected in any patient's distal biopsy set (table 2;  $p = 0.58$ ). The prevalence of sparse PMN infiltrates was negligible both at T1 (9/211; 4.2%) and T2 (12/211; 5.7%;  $p = 0.75$ ; not show in table).

*Histological subtyping and grading of oxyntic atrophy:* the score of each histological subtype of oxyntic atrophy is shown in table 3. At the time of the index endoscopy, non-metaplastic atrophy was present in 111/211 (52.6%) cases; in 59 of them it involved <30% of the oxyntic biopsy set. No significant score modifications were detected when the prevalence of atrophy at T1 and T2 were compared ( $p < 0.09$ ; table 3).

PPM was detected in the initial biopsy set (T1) in 200/211 (94.8%) cases (table 3B), while 160/211 (75.8%) cases showed IM (table 3C). At T2, 201/211 (95.2%) cases showed PPM. From

**Table 2** Mononuclear infiltrate in the oxyntic biopsy samples as obtained at T1 and T2 (A, B)

T1 oxyntic biopsy set Mononuclear infiltrate	A: T2 oxyntic biopsy set Mononuclear infiltrate ( $p = 0.43$ )				B: T2 antral biopsy set Mononuclear infiltrate ( $p = 0.58$ )			
	T2 N	T2 LG-M	T2 HG-M	Total	T2 N	T2 LG-M	T2 HG-M	Total
T1 N	0	0	0	0	152	34	0	186
T1 LG-M	0	93	57	150	19	6	0	25
T1 HG-M	0	34	27	61	0	0	0	0
TOTAL	0	127	84	211	171	40	0	211

The cells highlighted in grey shows cases that did not undergo any histological changes between T1 and T2. Cells in the space above and to the right of the grey cells show cases that worsened, whereas cells below and to the left of the grey cells show cases that underwent an improvement.

HG-M, high-grade mononuclear infiltrate; LG-M, low-grade mononuclear infiltrate; N, within normal limits; T1, time of the index biopsy set; T2, time of the last available biopsy check-up.

**Table 3** Atrophy in oxyntic (A, B, C, D) and antral (E, F) compartments over the follow-up time (T1: index biopsy set; T2: biopsy set at the end of the follow-up)

	A - Oxyntic atrophy: Non-metaplastic (p=0.09)					B - Oxyntic atrophy: Pseudo pyloric-metaplasia (p<0.001)				
	T2 G0	T2 G1	T2 G2	T2 G3	TOTAL	T2 G0	T2 G1	T2 G2	T2 G3	Total
T1 G0	58	42	0	0	100	3	7	1	0	11
T1 G1	51	59	0	0	110	5	27	11	9	52
T1 G2	0	1	0	0	1	1	8	20	16	45
T1 G3	0	0	0	0	0	1	10	31	61	103
Total	109	102	0	0	211	10	52	63	86	211
C - Oxyntic atrophy Intestinal metaplasia (p<0.001)	T2 G0	T2 G1	T2 G2	T2 G3	TOTAL	T2 G0	T2 G1	T2 G2	T2 G3	TOTAL
	T1 G0	24	22	3	2	51	3	5	0	0
T1 G1	7	73	25	5	110	2	12	3	7	24
T1 G2	1	12	14	5	32	3	0	3	10	16
T1 G3	0	7	3	8	18	1	2	9	151	163
TOTAL	32	114	45	20	211	9	19	15	168	211
E - Antral atrophy Non-metaplastic (p=1.000)	T2 G0	T2 G1	T2 G2	T2 G3	TOTAL	T2 G0	T2 G1	T2 G2	T2 G3	TOTAL
	T1 G0	202	6	0	0	208	200	11	0	0
T1 G1	3	0	0	0	3	0	0	0	0	0
T1 G2	0	0	0	0	0	0	0	0	0	0
T1 G3	0	0	0	0	0	0	0	0	0	0
TOTAL	205	6	0	0	211	200	11	0	0	211
F - Antral atrophy Intestinal metaplasia (p: not assessable)	T2 G0	T2 G1	T2 G2	T2 G3	TOTAL	T2 G0	T2 G1	T2 G2	T2 G3	TOTAL
	T1 G0	202	6	0	0	208	200	11	0	0
T1 G1	3	0	0	0	3	0	0	0	0	0
T1 G2	0	0	0	0	0	0	0	0	0	0
T1 G3	0	0	0	0	0	0	0	0	0	0
TOTAL	205	6	0	0	211	200	11	0	0	211

The cells highlighted in grey shows cases that did not undergo any histological changes between T1 and T2. Cells in the space above and to the right of the grey cells show cases that worsened, whereas cells below and to the left of the grey cells show cases that underwent an improvement. Histological atrophy score for biopsy set of the same gastric compartment; G0=no atrophic changes; G1=atrophy involving 1%–29% of the mucosal specimens; G2=30%–59%; G3= $\geq$ 60%.

T1 to T2, the PPM score decreased in 56/211 subjects (25.5%) and increased in 44/211 (20.8%) ( $p<0.001$ ); conversely, the IM score increased in 62/211 (29.4%) cases and decreased in 30/211 (14.2%) (table 3B–C;  $p<0.0001$ ).

Figure 2 shows the average score of each different histological phenotype seen in the oxyntic mucosa specimens at T1 and T2. While the mean percentage of non-atrophic oxyntic mucosa remained basically the same at T1 and T2 (19.6%, and 19.9%, respectively), the mean percentage of both non-metaplastic atrophy and PPM was higher at T1 than at T2, in contrast to

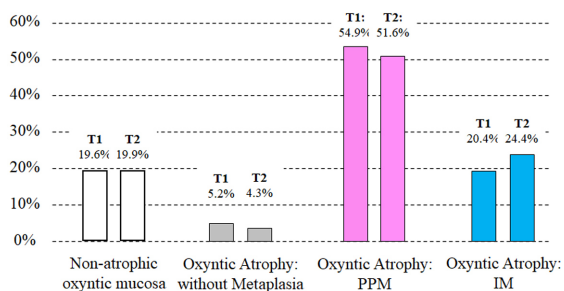


**Figure 2** Average score of different histological phenotypes of oxyntic gastric mucosa in 211 patients with autoimmune gastritis: significant negative correlation ( $-0.502$ ;  $p<0.001$ ) between pseudopyloric metaplasia (PPM) and intestinalised mucosa (IM). At T2, the average of the PPM decreases, mirroring the increasing average in the score of IM. Both native gastric mucosa and non-metaplastic atrophy showed no significant modifications in the average of the atrophy score at T1 versus T2. T1: oxyntic biopsy samples at the index biopsy; T2: oxyntic biopsy samples at the last check-up.

the higher prevalence of IM at T2 vs T1 (negative correlation between PPM and IM:  $-0.502$ ;  $p<0.0001$ ).

Table 3 shows the outcome of the global atrophy score (combining non-metaplastic, PPM, and IM) at T1 and T2. While the prevalence of any grade of atrophy at T1 and T2 was essentially the same (T1=203/211 (96.2%) vs T2=202/211 (95.7%)), the progression towards more severe atrophy grades was significant (progression: 25/211 (11.8%); regression 17/211 (8.0%);  $p<0.0001$ ).

*Histological subtyping and grading of antral/angular atrophy:* in the biopsy sets from the distal stomach (antrum, including the *incisura angularis*), the prevalence of atrophic lesions was negligible. Table 3 shows that both non-metaplastic and IM atrophic changes always involved less than 30% of the biopsy specimens (*ie*, grade 1).

*OLGA staging:* table 4 shows the OLGA stage at T1 and T2. There was no difference in the mean age of patients by stage ( $p=0.8763$  and  $0.1907$ , respectively). At both index and final check-up, most patients had stage II gastritis (179/211, and 175/211, respectively). There were no cases with OLGA stage IV. During the follow-up time, 179 of 211 patients (84.8%), 165 of whom had OLGA stage II, had no OLGA stage changes. A significant difference, however, emerged between the number of cases that progressed versus those that regressed (24/211 (11.4%) vs 8/211 (3.8%);  $p<0.0001$ ). At T2, due to the new occurrence of G1 atrophy in biopsy samples from the distal stomach (antrum or incisura), 10 cases had a stage III OLGA.

*ECL-cell status:* at T1, 20/211 (9.5%) patients had a normal ECL density and distribution; 167/211 (79.1%) patients had Diffuse-type (linear, or micronodular) hyperplasia; and 14 of 211 patients (6.6%) had adenomatoid hyperplasia/dysplasia;

**Table 4** OLGA stage of the 211 patients with autoimmune gastritis at the index endoscopy (T1) and at the last (T2) endoscopy/biopsy check-up ( $p < 0.00001$ )

OLGA stage At T1	OLGA stage at T2					Total
	Stage 0	Stage I	Stage II	Stage III	Stage IV	
Stage 0	3	5	0	0	0	8
Stage I	1	11	9	2	0	23
Stage II	3	3	165	8	0	179
Stage III	0	0	1	0	0	1
Stage IV	0	0	0	0	0	0
Total	7	19	175	10	0	211

The cells highlighted in grey shows cases that did not undergo any histological changes between T1 and T2. Cells in the space above and to the right of the grey cells show cases that worsened, whereas cells below and to the left of the grey cells show cases that underwent an improvement.

Type1 NETs were detected in 10/211 (4.7%) patients. At T2, the respective prevalence was: 24/211 (11.4%); 151/211 (71.6%); 25/211 (11.8%); 11/211 (5.2%). No neuroendocrine cancers were detected either at T1 or T2. At both T1 and T2, ECL-cell status correlated with both the score for oxyntic atrophy and the OLGA stage (table 5;  $p = 0.00001$ ).

At T1, there were three cases (1.4%) of linear/micronodular ECL-cell hyperplasia in the absence of oxyntic atrophy (table 5). The prevalence of ECL-cell diffuse and adenomatoid hyperplasia increased significantly along with an increasing oxyntic atrophy score, and all Type1 NETs clustered in the group of cases with atrophic changes involving more than 60% of the oxyntic biopsy specimens (table 5;  $p = 0.00001$ ).

Similarly, both adenomatoid ECL-cell hyperplasia and Type1 NET were significantly associated with OLGA Stage II. This suggests that, in AIG setting, OLGA stage II could be considered an indicator of high risk for Type1 NETs (table 5;  $p = 0.00001$ ).

### Neoplastic lesions (excluding NETs)

During the study period, no incident invasive gastric malignancies were detected. In December 2020, a further check of all participating patients with the Veneto Tumor Registry confirmed the absence of any GC after a cumulative follow-up of 10541 person years.

At T1, one polypoid lesion diagnosed as a low-grade intraepithelial gastric neoplasia (LG-IEN) was detected in a 47-year-old woman harbouring familial adenomatous polyposis (FAP). The LG-IEN relapsed twice during follow-up, was resected twice (apparently with IEN-free margins), but it was still present at the last check-up. Five more cases of LG-IEN emerged during the follow-up time: three were on the greater curvature; one on the posterior wall; no information is available on the location of remaining. Four of the five LG-IEN were removed endoscopically and had not relapsed after a follow-up of at least 18 months. The other LG-IEN was managed by non-radical endoscopic resection, and it was still present at the last follow-up, 22 months after its initial detection.

Based on data from the cancer registry (updated in December 2020), 25/211 patients developed incident extragastric primary malignancies in the following locations: breast (10 cases, all females); thyroid (5, all female); duodenum (2, both female); cutaneous melanoma (2, both males); kidney (1, female); liver (1, female); ovary (1); pancreas (1, male); urinary bladder (1, female); vulva (1). Standardised incident ratio (SIR) calculated for all these malignancies was 0.47 (95% CI 0.31 to 0.70). SIR was also calculated for the two most frequent primary cancer sites. The SIR for breast cancer did not demonstrate any excess risk (SIR=0.87; 95% CI 0.42 to 1.59), while for thyroid cancer it was marginally significant (SIR=3.09; 95% CI 1.001 to 7.20). All five primary thyroid malignancies were associated with follicular thyroiditis, as assessed histologically after surgical resection.

### DISCUSSION

The hypothesis providing momentum for this study was that the progression of AIG and its associated increased risk for GC reported by other researchers may have been affected by past or coexisting undetected *H. pylori* infection.<sup>9 10 40–45</sup> By assembling a homogeneous group of patients with suspected AIG in a single centre over a period of two decades, carefully selecting only those who met rigorous diagnostic criteria, and excluding past and present *H. pylori* infection with the most thorough testing currently available, we have monitored the mucosal changes and the development of preneoplastic lesions in a unique cohort of subjects with pure AIG.

Several of our findings require to be addressed in some detail: (1) the influence of AIG on epithelial malignancies; (2) the

**Table 5** Enterochromaffin-like-cell (ECL) cell status by the score of oxyntic atrophy score (A, B), and by OLGA stage (C, D)

ECL-N	A: Oxyntic atrophy score at T1 ( $p < 0.00001$ )					B: Oxyntic atrophy score at T2 ( $p < 0.00001$ )						
	G0	G1	G2	G3	Total	G0	G1	G2	G3	Total		
ECL-N	5	11	1	3	20	8	11	4	1	24		
ECL-DH	3	13	14	137	167	1	8	10	132	151		
ECL-AH/D	0	0	1	13	14	0	0	1	24	25		
T1-NET	0	0	0	10	10	0	0	0	11	11		
Total	8	24	16	163	211	9	19	15	168	211		
ECL-N	C: OLGA Stage at T1 ( $p < 0.00001$ )					D: OLGA Stage at T2 ( $p < 0.00001$ )						
	0	I	II	III	IV	T	0	I	II	III	IV	T
ECL-N	5	11	3	1	0	20	6	11	7	0	0	24
ECL-DH	3	12	152	0	0	167	1	8	133	9	0	151
ECL-AH/D	0	0	14	0	0	14	0	0	24	1	0	25
T1-NET	0	0	10	0	0	10	0	0	11	0	0	11
Total	8	23	179	1	0	211	7	19	175	10	0	211

The cells highlighted in grey shows cases that did not undergo any histological changes between T1 and T2. Cells in the space above and to the right of the grey cells show cases that worsened, whereas cells below and to the left of the grey cells show cases that underwent an improvement. T1: index biopsy set; T2: biopsy set at the end of the follow-up.

ECL (enterochromaffin like cell): ECL-status within normal limits; DH: diffuse hyperplasia (linear and nodular); AH/D: adenomatoid hyperplasia/dysplasia; T1-NET: Type 1 neuroendocrine tumours (NET). Histological atrophy score for the oxyntic biopsy set; G0=no atrophic changes; G1=atrophy involving 1%–29% of the mucosal specimens; G2=30%–59%; G3=≥60%.

progression of neuroendocrine proliferations; (3) the diagnostic impact of the biopsy sampling protocol; (4) phenotypes, scores and topography of inflammation and atrophy; and (5) the clinical relevance of staging gastritis.

### AIG on the development of epithelial malignancies

In contrast to other studies that have included AIG in the preneoplastic conditions, usually suggesting a risk slightly lower than that imparted by *H. pylori* infection, in our cohort of naïve *H. pylori*-negative patients neither high-grade IEN nor invasive GCs were detected during a follow-up time equivalent to 10 541 person years.<sup>9 10 41–47</sup>

Six cases of low-grade IEN were documented histologically. One case occurred and relapsed in a patient with FAP. A follow-up of >24 months revealed no relapse in four of the other five IEN cases after they underwent endoscopic resection at T1. The last IEN underwent non-radical resection at T1 and was confirmed as a low-grade at the last check-up (T2). Therefore, one can conclude that our study, with its rigorous exclusion of *H. pylori*-infected patients, has not revealed an association of AIG with excess of GC risk.

There was a mildly increased risk for thyroid cancer in women, suggesting that monitoring for the potential occurrence of thyroid disease in patients with AIG, particularly female, should be part of the management of AIG.<sup>48</sup> A corollary of this strategy is that patients with autoimmune thyroiditis and primary thyroid malignancies should undergo at the very least gastric functional serology (particularly gastrin 17) and cobalamin levels to screen for possible AIG. Both clinical follow-up and cross-checking with the Veneto Cancer Registry showed no increased incidence or any other malignancy in our study population.

### The progression of neuroendocrine proliferations

Only a few patients in our cohort (9.4% at T1 and 11.4% at T2) had a normal density and distribution of ECL-cells, as assessed by appropriate immunostaining. In these patients, the AIG diagnosis rested on the presence of PPM, which invariably coexists with corpus-restricted inflammation.

Diffuse (nodular and linear) hyperplastic lesions were the most prevalent, but a significant increase in adenomatoid hyperplasia/dysplasia was also documented from T1 (6.6%) to T2 (11.8%). Most cases occurred in subjects with extensive oxyntic mucosa atrophy (>60%), as did all Type1 NETs. The association between oxyntic atrophy and adenomatoid hyperplasia and NET is well established, as is the predictive value of adenomatoid hyperplasia/dysplasia in the development of NET.<sup>49</sup> In this study, the most reliable indicator of Type1 NET risk was the global score of oxyntic atrophy, which includes PPM and correlates well with ECL Adenomatoid hyperplasia/dysplasia. No Type1 NETs were detected in the absence of high-grade (>60%) oxyntic atrophy.<sup>49–51</sup>

In light of these confirmatory findings, we reiterate the importance of a representative biopsy sampling protocol when these patients undergo follow-up procedures. Pathologists should be reminded to use an immunohistochemical stain, such as synaptophysin or chromogranin A, to optimise the visualisation of the neuroendocrine components.

### The diagnostic impact of the biopsy sampling protocol

Without a biopsy protocol that provides separately identified sampling from both antrum and corpus, a diagnosis of AIG can often be suspected but not firmly established. In our study, all biopsy sets were compliant with the Updated Sydney System

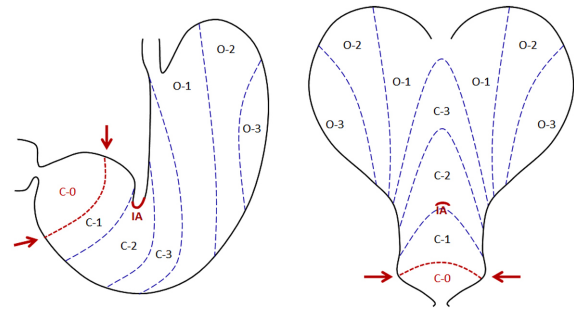


**Figure 3** Gastric location of the oxyntic-pyloric border, according to Kimura-Takemoto.<sup>55</sup> Evidence from Nakajima *et al* has documented that in *H. pylori*-naïve normal stomach ('without any findings of present or past *H. pylori* infection, inflammation, atrophy or intestinal metaplasia') the natively mucosecreting area (CO, in the figure) is located distally to the incisura angularis, the latter being originally lined by acid-producing oxyntic glands.<sup>58</sup> In 'primary' autoimmune gastritis, pyloric-type gastric glands at the incisura should be considered a metaplastic (pseudopyloric) transformation of the most distal oxyntic mucosa. On the left: stomach: anterior view. Right: stomach open along the greater curvature. The natively oxyntic stomach includes the mucosa of the incisura angularis (IA: in red *incisura angularis*). The figure also shows the two different patterns of atrophic gastritis in the model of *H. pylori* longstanding infection, the closed (C) and open (O) types. The figure is inspired by that published by Nakajima S, *et al. Dig Endosc* 2021;33:125–132<sup>58</sup> and modified according to the message delivered within the present manuscript.

protocol and included a sample from the *incisura angularis*. As recommended, this sample was placed in the same formalin vial as the antral specimens, because the *incisura* is considered part of the distal (*ie*, antral) gastric mucosa.<sup>52–54</sup> Our findings, however, suggest that this assumption needs to be critically revisited.

Endoscopic and histological studies from East Asia have reported on the variable location of the oxyntic-pyloric border (synonym: acid-alkaline border), not infrequently located distally to the landmark of the *incisura* (figure 3). A recent meticulously documented Japanese study has provided further evidence that the oxyntic mucosa may be natively located distally to the *incisura angularis* and extend up to the distal margin of the C1 mucosa area according to the Kimura and Takemoto classification (figure 3).<sup>2 55–58</sup>

This perspective of gastric compartmentalisation is very much keeping with the results of our study. In this cohort of *H. pylori*-naïve patients, one would not expect to find either inflammation or atrophy in the antral mucosa. However, we detected low-grade inflammation in 40 samples from the *incisura* and OLGA G1 atrophy in 11 of them. Although such specimens had been identified as being of antral origin because of their location, it is more likely that they originally consisted of natively oxyntic mucosa, inflamed and antralised by the autoimmune inflammatory process.<sup>56</sup> Immunophenotypic profiling of these specimens (using an anti-pepsinogen I immunostain) could have helped distinguish natively oxyntic from inflamed and atrophic mucosecreting gastric mucosa, but the limited availability of tissues when they were reviewed for the study made this step impossible. Nevertheless, considering the possibilities of confusion that specimens from the *incisura angularis* may cause, we suggest that their collection may be unnecessary, even unwarranted, for the diagnosis of AIG.

## Phenotypes, scores, and topography of inflammation and atrophy

Our study confirms that the non-atrophic variant of AIG (also referred to as ‘pre-atrophic’) can be encountered, although rarely.<sup>40</sup> Atrophy, once developed, appears to progress slowly, a finding that could support extending the interval of the endoscopy/biopsy follow-up. The inflammatory component in the oxyntic mucosa consisted almost exclusively of mononuclear cells, even arranged in nodular or follicular structures; in most patients, only rare and sparse eosinophils and neutrophils were found in the lamina propria.

At enrolment (T1), more than 94% of the oxyntic biopsy specimens showed PPM, with a prevalence that significantly exceeded that of IM (84.8%). This finding indicates that, PPM and corpus-restricted mononuclear inflammation, together with ECL diffuse and adenomatoid hyperplasia/dysplasia, should be considered the histological hallmarks of the atrophic AIG-stage.<sup>59–62</sup>

At the end of the follow-up, the average of the pseudopyloric score decreased inversely to the that of IM score (figure 2); this time-dependent dynamic modulation of different atrophy phenotypes further supports the hypothesis of a transformation from antralised to intestinalised epithelia.<sup>63–67</sup>

## The clinical relevance of staging gastritis

At both T1 and T2 timepoints, most cases (78.2%) featured OLGA-II gastritis stage. This finding indicates that—even in a long-term follow-up—the stage of atrophy progresses or regresses in only a minority of cases. The lack of progression is likely due to two main reasons: (1) at the time of the initial diagnosis corpus atrophy is already established; and (2) the restriction of atrophy to the oxyntic compartment does not promote a stage progression, which would require the expansion of inflammation and atrophy into the antral compartment.<sup>40 68</sup> When this happens in patients with AIG, concurrent *H. pylori* infection is most likely the underlying cause.

There was only one patient with OLGA stage III (0.5%) at T1, and 10 (4.7%) at T2. All cases clustering in OLGA-stage III (high-risk stage for epithelial malignancies) resulted from the concurrence of marked oxyntic atrophy with focal atrophic lesions in either antrum or *incisura*. Such a feature would suggest that some of the biopsy specimens submitted as antral/*incisural* were obtained from the most distal oxyntic mucosa, cranial to the Kimura and Takemoto oxyntic-pyloric border (figure 3).<sup>55 56</sup>

The prevalence of high-risk stages detected in the present study was almost half of that reported in a previous study of long-term AIG follow-up, in which the prevalence of stage III (8%) was potentially ascribed to the inclusion of a minority of patients with current or previous history of *H. pylori* infection.<sup>40</sup> In that study, however, *H. pylori* infection had not been excluded with the multiple rigorous methods we used in the present one. Yet, in neither series were there any patients with stage IV at any time point.

This study, which reports on the largest histologically confirmed adult cohort of patients with naïve *H. pylori*-negative AIG, has both limitations and strengths. Among the former are the lack of complete information on AIG comorbidities, which was available only for a subgroup of patients, and the absence of laboratory data on the gastric functional status, such as serology for gastrin 17 levels and pepsinogen ratios.<sup>69–71</sup> Although endoscopists who collected the biopsies used in this study were experienced with the Updated Sydney System protocol, we cannot exclude that some of the biopsy samples, particularly those supposed to originate from the *incisura angularis*, were obtained from a natively oxyntic compartment.

Its strengths include, in addition to its prospective design, the thorough exclusion of previous or current *H. pylori* infection, the length of the follow-up supported by a uniform histological protocol, a consistent histopathological evaluation, and the granular information on cancer incidence obtained from our regional cancer registry. Furthermore, the uniformity and stability of our study population minimised the influence that race, ethnicity and environment may have on the incidence and progression of AIG and its associated lesions.<sup>72</sup>

In conclusion, the present study fully characterises PPM, corpus restricted mononuclear infiltrate and ECL hyperplasia as histological hallmarks of AIG; furthermore, evidence is provided that corpus-restricted inflammation and atrophy have essentially no increased risk for GC compared with the general population. The cancer risk reported in other studies may have been enhanced by the presence of subjects with concurrent inflammatory and atrophic lesions in the mucosecreting gastric component (that is, the antrum), a phenotype characteristic of *H. pylori* infection.

**Twitter** Ludovica Bricca @BriccaLudovica

**Acknowledgements** The authors would like to thank Sonia Cesaro, Vanni Lazzarin, and Roberta Salmaso for their excellent technical assistance, and Gemma Maddalo for her contribution in clinical patients’ follow-up.

**Contributors** Conception and design: RMG, DYG and MR. Analysis and interpretation of the data: LB, MF, SG, MP, MR, DS and MZ. Critical revision of the manuscript for important intellectual content: APDT, FF, RMG, DYG, PM, MR, ES and MZ. Drafting of the article and final editing: RMG and MR. All authors reviewed the manuscript. Guarantor of the study: MR.

**Funding** The authors have not declared a specific grant for this research from any funding agency in the public, commercial or not-for-profit sectors.

**Competing interests** None declared.

**Patient and public involvement** Patients and/or the public were not involved in the design, or conduct, or reporting, or dissemination plans of this research.

**Patient consent for publication** Not applicable.

**Ethics approval** This study was conducted on anonymised archival material. Italian legislation identifies Cancer Registries as collectors of personal data for surveillance purposes without explicit individual consent. The authors do not require approval from a research ethics committee as the study was a descriptive analysis of individual data, without any direct or indirect intervention on patients.

**Provenance and peer review** Not commissioned; externally peer reviewed.

**Data availability statement** All data relevant to the study are included in the article or uploaded as supplementary information. All data relevant to the study are included in the article.

## ORCID iDs

Massimo Rugge <http://orcid.org/0000-0002-0679-0563>

Manuel Zorzi <http://orcid.org/0000-0001-6025-5214>

David Y Graham <http://orcid.org/0000-0002-6908-8317>

## REFERENCES

- 1 Sugano K, Tack J, Kuipers EJ, et al. Kyoto global consensus report on Helicobacter pylori gastritis. *Gut* 2015;64:1353–67.
- 2 Rugge M, Savarino E, Sbaraglia M, et al. Gastritis: the clinico-pathological spectrum. *Dig Liver Dis* 2021;53:1237–46.
- 3 Toh B-H. Diagnosis and classification of autoimmune gastritis. *Autoimmun Rev* 2014;13:459–62.
- 4 Lenti MV, Rugge M, Lahner E, et al. Autoimmune gastritis. *Nat Rev Dis Primers* 2020;6:56.
- 5 Neumann WL, Coss E, Rugge M, et al. Autoimmune atrophic gastritis—pathogenesis, pathology and management. *Nat Rev Gastroenterol Hepatol* 2013;10:529–41.
- 6 Fenwick S. On atrophy of the stomach. *The Lancet* 1870;96:78–80.
- 7 Torgersen J. Localization of gastritis and gastric cancer, especially in cases of pernicious anemia. *Acta radiol* 1944;25:845–55.
- 8 Magnus HA. A re-assessment of the gastric lesion in pernicious anaemia. *J Clin Pathol* 1958;11:289–95.
- 9 Strickland RG, Mackay IR. A reappraisal of the nature and significance of chronic atrophic gastritis. *Am J Dig Dis* 1973;18:426–40.
- 10 Morson BC, Sobin LH, Grundmann E, et al. Precancerous conditions and epithelial dysplasia in the stomach. *J Clin Pathol* 1980;33:711–21.



- 11 Veijola LI, Oksanen AM, Sipponen PI, *et al.* Association of autoimmune type atrophic corpus gastritis with *Helicobacter pylori* infection. *World J Gastroenterol* 2010;16:83–8.
- 12 Annibale B, Azzoni C, Corleto VD, *et al.* Atrophic body gastritis patients with enterochromaffin-like cell dysplasia are at increased risk for the development of type gastric carcinoid. *Eur J Gastroenterol Hepatol* 2001;13:1449–56.
- 13 Misiewicz JJ. The Sydney system: a new classification of gastritis. Introduction. *J Gastroenterol Hepatol* 1991;6:207–8.
- 14 Price AB. The Sydney system: histological division. *J Gastroenterol Hepatol* 1991;6:209–22.
- 15 Dixon MF, Genta RM, Yardley JH, *et al.* Classification and grading of gastritis. The updated Sydney system. International workshop on the histopathology of gastritis, Houston 1994. *Am J Surg Pathol* 1996;20:1161–81.
- 16 Miceli E, Vanoli A, Lenti MV, *et al.* Natural history of autoimmune atrophic gastritis: a prospective, single centre, long-term experience. *Aliment Pharmacol Ther* 2019;50:1172–80.
- 17 Lash RH, Genta RM. Routine anti-*Helicobacter* immunohistochemical staining is significantly superior to reflex staining protocols for the detection of *Helicobacter* in gastric biopsy specimens. *Helicobacter* 2016;21:581–5.
- 18 Rugge M, Sacchi D, Genta RM, *et al.* Histological assessment of gastric pseudopyloric metaplasia: intra- and inter-observer consistency. *Dig Liver Dis* 2021;53:61–5.
- 19 Rugge M, Correa P, Dixon MF, *et al.* Gastric mucosal atrophy: interobserver consistency using new criteria for classification and grading. *Aliment Pharmacol Ther* 2002;16:1249–59.
- 20 Ruiz B, Garay J, Johnson W, *et al.* Morphometric assessment of gastric antral atrophy: comparison with visual evaluation. *Histopathology* 2001;39:235–42.
- 21 Goldenring JR, Nam KT, Wang TC, *et al.* Spasmolytic polypeptide-expressing metaplasia and intestinal metaplasia: time for reevaluation of metaplasias and the origins of gastric cancer. *Gastroenterology* 2010;138:2207–10.
- 22 Rugge M. Biologic profiles meet clinical priorities: incorporating pseudopyloric, and spasmolytic-expressing metaplasia in the assessment of gastric atrophy. *Virchows Arch* 2020;477:487–8.
- 23 Rugge M, Genta RM, Graham DY, *et al.* Chronicles of a cancer foretold: 35 years of gastric cancer risk assessment. *Gut* 2016;65:721–5.
- 24 Correa P, Piazuelo MB, Wilson KT. Pathology of gastric intestinal metaplasia: clinical implications. *Am J Gastroenterol* 2010;105:493–8.
- 25 Spechler SJ, Merchant JL, Wang TC, *et al.* A summary of the 2016 James W. Freston conference of the American gastroenterological association: intestinal metaplasia in the esophagus and stomach: origins, differences, similarities and significance. *Gastroenterology* 2017;153:e6–13.
- 26 Rugge M, Correa P, Di Mario F, *et al.* OLGA staging for gastritis: a tutorial. *Dig Liver Dis* 2008;40:650–8.
- 27 Rugge M, Pennelli G, Pilozi E, *et al.* Gastritis: the histology report. *Dig Liver Dis* 2011;43 Suppl 4:S373–84.
- 28 Vanoli A, La Rosa S, Miceli E, *et al.* Prognostic evaluations tailored to specific gastric neuroendocrine neoplasms: analysis of 200 cases with extended follow-up. *Neuroendocrinology* 2018;107:114–26.
- 29 Kushima R, Lauwers GY, Rugge M. Gastric Dysplasia. In: *WHO classification of tumours editorial board: digestive system tumours*. 5th Ed. Lyon: International Agency for Research on Cancer, 2019: 71–5.
- 30 Carneiro F, Fukayama M, Grabsch H. Gastric adenocarcinoma. In: *WHO classification of tumours editorial board: digestive system tumours*. 5th Ed. Lyon: International Agency for Research on Cancer, 2019: 85–95.
- 31 Landis JR, Koch GG. The measurement of observer agreement for categorical data. *Biometrics* 1977;33:159–74.
- 32 Mégraud F, Floch P, Labenz J, *et al.* Diagnostic of *Helicobacter pylori* infection. *Helicobacter* 2016;21 Suppl 1:8–13.
- 33 Best LM, Takwoingi Y, Siddique S, *et al.* Non-Invasive diagnostic tests for *Helicobacter pylori* infection. *Cochrane Database Syst Rev* 2018;3:CD012080.
- 34 Makrathathis A, Hirschl AM, Mégraud F, *et al.* Review: diagnosis of *Helicobacter pylori* infection. *Helicobacter* 2019;24 Suppl 1:e12641.
- 35 Syrjänen K, Eskelinen M, Peetsalu A, *et al.* GastroPanel® Biomarker Assay: The Most Comprehensive Test for *Helicobacter pylori* Infection and Its Clinical Sequelae. A Critical Review. *Anticancer Res* 2019;39:1091–104.
- 36 Chung WC, Jeon EJ, Oh JH, *et al.* Dual-Priming oligonucleotide-based multiplex PCR using tissue samples from the rapid urease test kit for the detection of *Helicobacter pylori* in bleeding peptic ulcers. *Dig Liver Dis* 2016;48:899–903.
- 37 Kiss S, Zsikla V, Frank A, *et al.* *Helicobacter*-negative gastritis: polymerase chain reaction for *Helicobacter* DNA is a valuable tool to elucidate the diagnosis. *Aliment Pharmacol Ther* 2016;43:924–32.
- 38 Registrotumoriveneto. Available: <https://www.registrotumoriveneto.it/it/>
- 39 . SAS EG v.6.1. Cary, NC, USA SAS Institute Inc..
- 40 Rugge M, Fassan M, Pizzi M, *et al.* Autoimmune gastritis: histology phenotype and OLGA staging. *Aliment Pharmacol Ther* 2012;35:1460–6.
- 41 Vannella L, Lahner E, Osborn J, *et al.* Systematic review: gastric cancer incidence in pernicious anaemia. *Aliment Pharmacol Ther* 2013;37:375–82.
- 42 Rugge M, Fassan M, Pizzi M, *et al.* Letter: gastric cancer and pernicious anaemia—often *Helicobacter pylori* in disguise. *Aliment Pharmacol Ther* 2013;37:764–5.
- 43 Bizzaro N, Antico A, Villalta D. Autoimmunity and gastric cancer. *Int J Mol Sci* 2018;19:377.
- 44 Lahner E, Capasso M, Carabotti M, *et al.* Incidence of cancer (other than gastric cancer) in pernicious anaemia: a systematic review with meta-analysis. *Dig Liver Dis* 2018;50:780–6.
- 45 Lahner E, Zagari RM, Zullo A, *et al.* Chronic atrophic gastritis: Natural history, diagnosis and therapeutic management. A position paper by the Italian Society of Hospital Gastroenterologists and Digestive Endoscopists [AIGO], the Italian Society of Digestive Endoscopy [SIED], the Italian Society of Gastroenterology [SIGE], and the Italian Society of Internal Medicine [SIMI]. *Dig Liver Dis* 2019;51:1621–32.
- 46 Song M, Latorre G, Ivanovic-Zivic D, *et al.* Autoimmune diseases and gastric cancer risk: a systematic review and meta-analysis. *Cancer Res Treat* 2019;51:841–50.
- 47 Zádori N, Szakó L, Vánca S, *et al.* Six autoimmune disorders are associated with increased incidence of gastric cancer: a systematic review and meta-analysis of half a million patients. *Front Immunol* 2021;12:750–3.
- 48 Venerito M, Link A, Rokkas T, *et al.* Gastric cancer - clinical and epidemiological aspects. *Helicobacter* 2016;21 Suppl 1:39–44.
- 49 Solcia E, Rindi G, Larosa S, *et al.* Morphological, molecular, and prognostic aspects of gastric endocrine tumors. *Microsc Res Tech* 2000;48:339–48.
- 50 Vanoli A, La Rosa S, Luinetti O, *et al.* Histologic changes in type a chronic atrophic gastritis indicating increased risk of neuroendocrine tumor development: the predictive role of dysplastic and severely hyperplastic enterochromaffin-like cell lesions. *Hum Pathol* 2013;44:1827–37.
- 51 Nehme F, Rowe K, Palko W, *et al.* Autoimmune metaplastic atrophic gastritis and association with neuroendocrine tumors of the stomach. *Clin J Gastroenterol* 2020;13:299–307.
- 52 Hunt RH, Camilleri M, Crowe SE, *et al.* The stomach in health and disease. *Gut* 2015;64:1650–68.
- 53 Van Zanten SJ, Dixon MF, Lee A. The gastric transitional zones: neglected links between gastroduodenal pathology and *Helicobacter* ecology. *Gastroenterology* 1999;116:1217–29.
- 54 Xia HH, Kalantar JS, Talley NJ, *et al.* Antral-type mucosa in the gastric incisura, body, and fundus (antralization): a link between *Helicobacter pylori* infection and intestinal metaplasia? *Am J Gastroenterol* 2000;95:114–21.
- 55 Kimura K, Takemoto T. An endoscopic recognition of the atrophic border and its significance in chronic gastritis. *Endoscopy* 1969;3:87–97.
- 56 Kimura K. Chronological transition of the fundic-pyloric border determined by stepwise biopsy of the lesser and greater curvatures of the stomach. *Gastroenterology* 1972;63:584–92.
- 57 Rugge M, Sacchi D, Graham DY, *et al.* Secondary prevention of gastric cancer: merging the endoscopic atrophic border with OLGA staging. *Gut* 2020;69:1151–2.
- 58 Nakajima S, Watanabe H, Shimbo T, *et al.* Incisura angularis belongs to fundic or transitional gland regions in *Helicobacter pylori*-naïve normal stomach: Sub-analysis of the prospective multi-center study. *Dig Endosc* 2021;33:125–32.
- 59 Goldenring JR. Pyloric metaplasia, pseudopyloric metaplasia, ulcer-associated cell lineage and spasmolytic polypeptide-expressing metaplasia: reparative lineages in the gastrointestinal mucosa. *J Pathol* 2018;245:132–7.
- 60 Venerito M, Varbanova M, Röhl F-W, *et al.* Oxyntic gastric atrophy in *Helicobacter pylori* gastritis is distinct from autoimmune gastritis. *J Clin Pathol* 2016;69:677–85.
- 61 Choudhuri J, Hall S, Castrodad-Rodriguez CA, *et al.* Features that aid identification of autoimmune gastritis in a background of active *Helicobacter pylori* infection. *Arch Pathol Lab Med* 2021;145:1536–43.
- 62 Jeong S, Choi E, Petersen CP, *et al.* Distinct metaplastic and inflammatory phenotypes in autoimmune and adenocarcinoma-associated chronic atrophic gastritis. *United European Gastroenterol J* 2017;5:37–44.
- 63 Mills JC, Goldenring JR. Metaplasia in the stomach arises from gastric chief cells. *Cell Mol Gastroenterol Hepatol* 2017;4:85–8.
- 64 Jin RU, Mills JC. Are gastric and esophageal metaplasias relatives? the case for Barrett's Stemming from SPEM. *Dig Dis Sci* 2018;63:2028–41.
- 65 Graham DY, Zou WY. Guilt by association: intestinal metaplasia does not progress to gastric cancer. *Curr Opin Gastroenterol* 2018;34:458–64.
- 66 Graham DY, Rugge M, Genta RM. Diagnosis: gastric intestinal metaplasia - what to do next? *Curr Opin Gastroenterol* 2019;35:535–43.
- 67 Goldenring JR, Mills JC, Plasticity C. Cellular plasticity, reprogramming, and regeneration: metaplasia in the stomach and beyond. *Gastroenterology* 2022;162:415–30.
- 68 Salazar BE, Pérez-Cala T, Gomez-Villegas SI, *et al.* The OLGA-OLGIM staging and the interobserver agreement for gastritis and preneoplastic lesion screening: a cross-sectional study. *Virchows Arch* 2022;480:759–69.
- 69 Agrés L, Kuipers EJ, Kupcinskis L, *et al.* Rationale in diagnosis and screening of atrophic gastritis with stomach-specific plasma biomarkers. *Scand J Gastroenterol* 2012;47:136–47.
- 70 Di Mario F, Crafa P, Barchi A, *et al.* Pepsinogen II in gastritis and *Helicobacter pylori* infection. *Helicobacter* 2022;27:e12872.
- 71 Kishikawa H, Nakamura K, Ojiri K, *et al.* Relevance of pepsinogen, gastrin, and endoscopic atrophy in the diagnosis of autoimmune gastritis. *Sci Rep* 2022;12:4202.
- 72 Choi CE, Sonnenberg A, Turner K, *et al.* High prevalence of gastric preneoplastic lesions in East Asians and Hispanics in the USA. *Dig Dis Sci* 2015;60:2070–6.